Assessing Machine Learning for LEO Satellite Orbit Determination in Simultaneous Tracking and Navigation

Trier Mortlock
Department of Mechanical and Aerospace Engineering
University of California, Irvine
Irvine, CA 92697
tmortloc@uci.edu

Zaher M. Kassas
Department of Mechanical and Aerospace Engineering
Department of Electrical Engineering and Computer Science
University of California, Irvine
Irvine, CA 92697
zkassas@ieee.org

2021 IEEE Aerospace Conference | 978-1-7281-7436-5/21/$31.00 ©2021 IEEE | DOI: 10.1109/AERO50100.2021.9438144

Abstract— **Machine learning for orbit determination of low Earth orbit (LEO) satellites in a simultaneous tracking and navigation (STAN) framework is assessed. STAN is a navigation paradigm that aims to exploit LEO satellites, which are not intended for navigation purposes. Since these satellites are not intended as navigation sources, their states (position, velocity, clock bias, and clock drift) cannot be assumed to be transmitted to the navigator. STAN estimates the states of such satellites simultaneously with the states of the navigating vehicle, using Doppler and pseudorange measurements drawn from the LEO satellite signals. This paper proposes a machine learning algorithm for predicting LEO satellite orbits in the STAN framework. A time delay neural network (TDNN) is developed, which is shown to improve the LEO satellite tracking performance over an extended Kalman filter (EKF)-based satellite tracking approach. The proposed EKF-TDNN-STAN is validated experimentally on a ground vehicle, where the Doppler measurements extracted from two Orbcomm LEO satellite signals were used to aid an on-board inertial measurement unit. In the experiment, the vehicle navigated for a total of 258 seconds, the last 30 seconds of which were in the absence of global navigation satellite system (GNSS) signals. The vehicle traversed a distance of 1.1 km during the period of GNSS unavailability. An EKF-STAN achieved a ground vehicle three-dimensional (3-D) position root mean-squared error (RMSE) of 10.6 m, while the two LEO satellites were tracked with 3-D position RMSE of 71 m and 26 m, respectively. In contrast, the proposed EKF-TDNN-STAN framework achieved a ground vehicle 3-D position root RMSE of 6.6 m, while the two LEO satellites were tracked with 3-D position RMSE of 6 m and 26 m, respectively.**

TABLE OF CONTENTS

U.S. Government work not protected by U.S. copyright

1. INTRODUCTION

Historically, the consistent focus in the study of space has been to go further: exploring new planets and stars, probing deeper into the vast expanse that surrounds the Earth. But recently, many have turned their attention not deeper into space, but closer—towards lower orbital altitudes around the Earth. The astronomic rise in the deployment of commercial low Earth orbit (LEO) satellites over the past years is well documented [1]. The concept of large LEO satellite constellations is not new; however, recent developments in satellite technologies and reduction in launch costs, among other factors, have been key enablers for the rapid proliferation of successful LEO satellite constellations. Older communication-based LEO constellations like Orbcomm, Iridium, and Globalstar, are welcoming a new wave of thousands of broadband internet-based megaconstellations, funded by major companies like SpaceX, Amazon, and Boeing [2], [3]. This rapidly developing commercial frontier around the Earth's atmosphere has many different players involved, from government and defense agencies, to private corporations, to international competitors.

As with many scientific developments, there are other unintended benefits of this quick race for dominance in LEO space. One such example is in the field of opportunistic navigation, wherein signals not specifically designed for navigation can be exploited for positioning, navigation, and timing (PNT) purposes [4]. Although the main goals of the majority of the LEO constellations may be for broadband internet coverage, communications, or defense applications, signals from LEO satellites can be used opportunistically in navigation systems, under the right circumstances [5], [6], [7]. LEO satellite signals offer unique advantages over global navigation satellite system (GNSS) signals, namely: (i) stronger signal power because of the lower orbital altitude, (ii) diversity in geometry and frequency, and (iii) increased availability due to abundance of satellites. Furthermore these advantages come at no cost for an opportunistic receiver—they are free to use with the proper equipment as downlink signals can be exploited with no subscriptions required.

However, the use of LEO satellites for opportunistic navigation purposes poses some inherent challenges. For example, unlike GNSS satellites, LEO satellites cannot be assumed to transmit precise ephemerides which allows extracting satellite position states. Although the Keplerian elements parameterizing the orbits of these LEO satellites are made publicly available by the North American Aerospace Defense

Authorized licensed use limited to: ISRO Telemetry Tracking and Command Network. Downloaded on May 11,2023 at 11:39:21 UTC from IEEE Xplore. Restrictions apply.

Command (NORAD) and are updated daily in the two-line element (TLE) files [8], the resulting accuracy in the satellite position and velocity states when using orbit determination software and TLE files (e.g., simplified general perturbations 4 [9]) is in the order of a few kilometers and a few meters per second, respectively. One approach to alleviate such uncertainty is the use of differential LEO navigation frameworks [10], [7]. Moreover, the extraction of navigation observables from LEO satellite signals is not yet fully understood, partly because very little is known about future LEO constellation signals. One approach to deal with such lack of knowledge is blind techniques [11], [12], [13], [14], [15], [16]. This paper addresses the challenge of imprecise knowledge of the LEO satellite states via the simultaneous tracking and navigation (STAN) framework, where the LEO satellite states are tracked while simultaneously using their signals for navigation [17].

An extended Kalman filter (EKF)-based STAN framework requires a dynamics model to propagate the state estimates and corresponding estimation uncertainties of LEO satellites. While several orbital models were investigated for the STAN framework [18], [19], [20], machine learning-based approaches were not considered. In this paper, a time delay neural network (TDNN) is developed to aid in the determination of the LEO satellite positions in the STAN framework. By employing machine learning, the aim is to improve the filter's ability to estimate the LEO satellite positions. Machine learning models possess the ability to learn complex nonlinear dynamics models with high levels of uncertainty, and make accurate predictions at a fraction of the computational cost of comparable orbit propagation methods. During times of GNSS signal availability, the machine learning model will be trained on the data as the vehicle tracks the LEO satellites, and after GNSS signals are no longer available, the machine learning aided LEO propagation model will produce predictions of the LEO satellite states within the STAN framework, leading to a higher degree of accuracy in the vehicle's navigation solution.

The rest of the paper is organized as follows. Section 2 gives an overview of the EKF-based STAN framework. Section 3 formulates the machine learning approach for LEO satellite predictions. Section 3 presents experimental results of a ground vehicle navigating via the EKF-TDNN-STAN framework and compares the navigation performance to an EKF-based STAN approach. Section 5 gives concluding remarks.

2. EKF-STAN Framework Overview

This section outlines the STAN framework used to estimate the states of the navigating vehicle and the dynamic, stochastic states of LEO satellites. At its core, STAN is an opportunistic navigation framework that works in two primary modes: (i) when GNSS satellites are available, the navigating tracks the LEO satellite states; and (ii) when GNSS satellites become unavailable, the navigating vehicle uses the LEO satellites signals to estimate its own state, while simultaneously tracking the LEO satellites. STAN can be thought of as a generalization of radio simultaneous and mapping (radio SLAM) [21], [22], [23], [24], [25], in which the radio transmitters (here, LEO satellites) are non-stationary. STAN employs a traditional EKF as diagramed in Figure 1. The conventional STAN framework will be referred to as EKF-STAN.

In a traditional GNSS-aided inertial navigation system (INS), when GNSS is unavailable, the vehicle relies solely on its inertial measurement unit (IMU) [26]. An IMU consists of a triad gyroscope and triad accelerometer that make specific force and rotation rate measurements to relate the vehicle's orientation and position in the body frame to a local or global frame. The IMU provides short-term positioning updates but errors in the measurements can quickly accumulate through integration. For this reason, during GNSS-outages, the LEO satellites provide measurements to help correct the drifting behavior of the IMU. In STAN, the state vector of the system is defined as

$$\boldsymbol{x} = \left[\, \boldsymbol{x}_{\mathrm{r}}^{\mathsf{T}},\, \boldsymbol{x}_{\mathrm{leo}_1}^{\mathsf{T}},\, \ldots,\, \boldsymbol{x}_{\mathrm{leo}_{\mathrm{M}}}^{\mathsf{T}} \right]^{\mathsf{T}} \tag{1}$$

$$\boldsymbol{x}_{\mathrm{r}} = \left[\, {}^{B}_{G}\bar{\boldsymbol{q}}^{\mathsf{T}},\, \boldsymbol{r}_{\mathrm{r}}^{\mathsf{T}},\, \dot{\boldsymbol{r}}_{\mathrm{r}}^{\mathsf{T}},\, \boldsymbol{b}_{\mathrm{g}}^{\mathsf{T}},\, \boldsymbol{b}_{\mathrm{a}}^{\mathsf{T}},\, c\delta t_{\mathrm{r}},\, c\dot{\delta t}_{\mathrm{r}} \right]^{\mathsf{T}} \tag{2}$$

$$\boldsymbol{x}_{\mathrm{leo}_{\mathrm{m}}} = \left[\, \boldsymbol{r}_{\mathrm{leo}_{\mathrm{m}}}^{\mathsf{T}},\, \dot{\boldsymbol{r}}_{\mathrm{leo}_{\mathrm{m}}}^{\mathsf{T}},\, c\delta t_{\mathrm{leo}_{\mathrm{m}}},\, c\dot{\delta t}_{\mathrm{leo}_{\mathrm{m}}} \right]^{\mathsf{T}}, \tag{3}$$

where $\boldsymbol{x}_{\mathrm{r}}$ is the state vector of the vehicle consisting of ${}^{B}_{G}\bar{\boldsymbol{q}}$: a four-dimensional (4-D) unit quaternion representing the orientation of a body frame B fixed at the IMU with respect to a global frame G; $\boldsymbol{r}_{\mathrm{r}}$ and $\dot{\boldsymbol{r}}_{\mathrm{r}}$: three-dimensional (3-D) position and velocity vectors, respectively, of the vehicle; $\boldsymbol{b}_{\mathrm{g}}$ and $\boldsymbol{b}_{\mathrm{a}}$: 3-D biases of the IMU's gyroscope and accelerometer, respectively; δt_{r} and $\dot{\delta t}_{\mathrm{r}}$: clock bias and drift of the receiver, respectively; and c being the speed of light. The vector $\boldsymbol{x}_{\mathrm{leo}_{\mathrm{m}}}$ is the state vector of the m^{th} LEO satellite, consisting of $\boldsymbol{r}_{\mathrm{leo}_{\mathrm{m}}}$ and $\dot{\boldsymbol{r}}_{\mathrm{leo}_{\mathrm{m}}}$: 3-D satellite position and velocity; $\delta t_{\mathrm{leo}_{\mathrm{m}}}$ and $\dot{\delta t}_{\mathrm{leo}_{\mathrm{m}}}$: satellite's transceiver clock bias and drift, respectively; and $m = 1, \ldots, M$, with M being the total number of LEO satellites used.

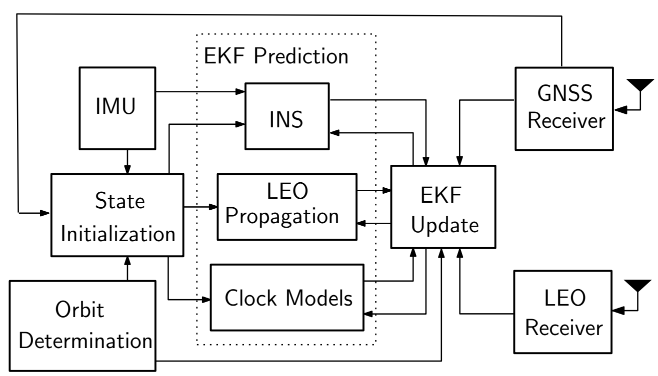

Figure 1. EKF-STAN framework that uses LEO satellite signals and GNSS signals (when available) to simultaneously track that states of LEO satellites while aiding a vehicle's inertial navigation system (INS).

The EKF performs a time update of the vehicle's position, velocity, and orientation using measurements from the IMU processed with the strapdown INS kinematic equations [27]. The vehicle's accelerometer and gyroscope biases are modeled to evolve according to a velocity random walk model. The clock states of the vehicle and LEO satellites are modeled to evolve according to the standard double integrator model driven by noise. The LEO satellite position and velocity are predicted through a two-body with J_2 propagation model, where J_2 is the second gravitational zonal coefficient [20]. During the EKF update, the vehicle-mounted LEO satellite receiver makes pseudorange measurements ρ and/or Doppler frequency measurements f_D on the transmitted LEO satellite signals based on the known frequency profiles of the satellites of interest. A pseudorange rate measurement $\dot{\rho}$ can be

Authorized licensed use limited to: ISRO Telemetry Tracking and Command Network. Downloaded on May 11,2023 at 11:39:21 UTC from IEEE Xplore. Restrictions apply.

obtained from f_D according to $\dot{\rho} = -\frac{c}{f_c} f_D$, where f_c is the carrier frequency. The pseudorange measurement, $\rho_{\mathrm{leo_m}}$, at time-step j from the m^{th} LEO satellite is modeled according to

$$\rho_{\mathrm{leo_m}}(j) = \|\boldsymbol{r}_{\mathrm{r}}(j) - \boldsymbol{r}_{\mathrm{leo_m}}(j)\|_2 + c \cdot [\delta t_{\mathrm{r}}(j) - \delta t_{\mathrm{leo_m}}(j)] + v_{\mathrm{leo_m}}(j), \quad j = 1, 2, \ldots, \tag{4}$$

where the ionospheric delays are ignored due to the high frequency of the transmitted signals (most LEO megaconstellations will transmit in the K band and above), tropospheric delays are also ignored due to their negligible effects compared to the LEO satellite position and velocity estimate errors [28], and v_{leo_m} is the measurement noise, which is modeled as a white Gaussian random sequence with variance $\sigma^2_{\rho_{\mathrm{leo,m}}}$ [3].

The LEO receiver can also make pseudorange rate measurements, $\dot{\rho}_{\mathrm{leo}_m}$, on the LEO satellites which are modeled following the same above assumptions as

$$\dot{\rho}_{\mathrm{leo}_m}(j) = [\dot{\boldsymbol{r}}_{\mathrm{leo}_m}(j) - \dot{\boldsymbol{r}}_r(j)]^{\mathsf{T}} \frac{[\boldsymbol{r}_r(j) - \boldsymbol{r}_{\mathrm{leo}_m}(j)]}{\|\boldsymbol{r}_r(j) - \boldsymbol{r}_{\mathrm{leo}_m}(j)\|_2} + c \cdot [\dot{\delta} t_r(j) - \dot{\delta} t_{\mathrm{leo}_m}(j)] + v_{\dot{\rho}_m}(j), \quad j = 1, 2, \ldots, \tag{5}$$

where $v_{\dot{\rho}_m}$ is the measurement noise, which is modeled as a white Gaussian random sequence with variance $\sigma^2_{\dot{\rho}_{\mathrm{leo,m}}}$ [29].

LEO Orbit Determination

Orbit determination, which is crucial to the STAN framework's performance, is a well-studied topic in the field of space situational awareness (SSA) [30], [31], [32], [33], [34]. Notable orbit propagation models fall into two main categories: (i) numerical: high-fidelity models that attempt to include all relevant forces and numerically integrate the satellite equations of motion and (ii) analytical: low-fidelity models that approximate some forces while disregarding others. The difference between these categories is the trade-off between accuracy and computational complexity: (i) analytical propagators achieve a computationally efficient analytical solution by reducing model fidelity, which in turn degrades the propagation accuracy, while (ii) numerical propagators achieve higher accuracy by performing computationally costly numerical integrations of complicated force models. The equation of motion of the perturbed satellite problem can be described as

$$\ddot{\boldsymbol{r}} = -\frac{\mu}{\|\boldsymbol{r}\|_2^3} \boldsymbol{r} + \boldsymbol{f}, \tag{6}$$

where $\boldsymbol{r}$ is the position vector of the satellite, $\|\boldsymbol{r}\|_2$ is the distance between the satellite and the center of the Earth, μ is the gravitational constant scaled by the masses of the Earth and satellite, and $\boldsymbol{f}$ is the perturbing force where

$$\boldsymbol{f} = \boldsymbol{f}_{NS} + \boldsymbol{f}_{3B} + \boldsymbol{f}_g + \boldsymbol{f}_{Drag} + \boldsymbol{f}_{SRP} + \boldsymbol{f}_{ERP} + \boldsymbol{f}_{Other},$$

where the above forces represent perturbation effects of the mass distribution and tidal effects ($\boldsymbol{f}_{NS}$), third body effects ($\boldsymbol{f}_{3B}$), general relativity ($\boldsymbol{f}_g$), atmospheric resistance ($\boldsymbol{f}_{Drag}$), solar radiation pressure ($\boldsymbol{f}_{SRP}$), Earth radiation pressure ($\boldsymbol{f}_{ERP}$), and other factors such as thermal forces, magnetically induced forces, misalignment effects and more($\boldsymbol{f}_{Other}$) [35]. Depending on the propagation model used, some of these forces are lumped together while others are explicitly calculated, all of which are factors that affect the propagation accuracy.

One example of an analytical satellite propagator, known as the simplified general perturbations 4 (SGP4) model, uses TLE files, produced daily by the NORAD, that contain orbital elements and corrective terms to initialize and propagate the position and velocity of a satellite [8]. However, the simplified models of perturbing forces cause errors in a propagated satellite orbit around three to ten kilometers, 24-hours after a TLE is produced [9]. In contrast, numerical propagators, also known as precise orbit determination (POD) methods, yield accurate ephemerides with errors on the order of tens-of-meters in the radial, along-track, and cross-track directions for a satellite, with more error occurring in the along-track direction [9], [36]. Unlike SGP4 propagators, POD propagators do not have a TLE-equivalent initialization file that is publicly available. Some studies have looked at the use of TLEs with POD methods [37], [38], while others do not mention where the initial conditions of the integrators are determined from. In general, most newer developments of POD methods for satellites focus on improving previously developed algorithms [39]. There has been some recent work for satellite propagation methods focused on short-time propagation periods for real-time applications [40], [41], [42]. For compatibility with the STAN framework, lower-fidelity analytical models have been studied most extensively, although the specific context in which STAN operates in LEO satellite orbit propagation is largely unexplored. The LEO propagation model used under the EKF-STAN results later in this paper is the standard two-body propagation model outlined in [20]. Numerous recent studies have focused on using machine learning to aid orbit determination techniques. These sources have explored different machine learning algorithms and showed promising results in improving LEO satellite orbit determination accuracy.

3. Machine Learning for LEO Predictions

Machine learning has been utilized for a wide variety of scientific and engineering problems that have high dynamics and uncertainties. One branch of machine learning involves the employment of neural network models that can attempt to learn trends in data and make predictions or inferences based on this learning process. The three main types of learning problems are (i) supervised learning: a model is trained on samples and their corresponding outputs, (ii) unsupervised learning: a model is only given inputs, and (iii) reinforcement learning: a model makes multi-stage decisions and rewards. Many studies have examined machine learning applications in the context of orbit determination, LEO satellites, and/or SSA applications. In [43], the initial orbit determination problem was explored using stationary ground stations and training data for a month-long period. Learning via distribution regression for robust orbit determination was explored along with the transfer learning system for multiple-spacecraft scenarios [44], [45]. In [46], a convolutional neural network was developed for space object pattern classification in a game theoretic approach. The orbit prediction of LEO space debris was studied via machine learning models in [47]. Improving satellite orbit accuracy was studied through the use of support vector machines in [48], [49], [50]. Deep learning techniques using recurrent neural networks were utilized to

Authorized licensed use limited to: ISRO Telemetry Tracking and Command Network. Downloaded on May 11,2023 at 11:39:21 UTC from IEEE Xplore. Restrictions apply.

model satellite behaviors and maneuvers and satellite orbit propagation [51], [52].

The STAN framework's estimation of the dynamic and stochastic states of the LEO satellites proves a difficult challenge, especially with only one navigating vehicle. Apart from issues of observability and consistency, the framework performance is highly dependent on the orbit propagation model used for the LEO satellites. Unlike multi-day/week centric orbit determination in SSA, STAN can operate efficiently with orbit propagation lengths for LEO satellites in the order of minutes. The case of using machine learning to aid the short-term orbit propagation of LEO satellites is largely unexplored. Ideally under STAN, when the vehicle has access to GNSS satellites, it knows its current position to a high degree of accuracy and can begin to map the moving LEO satellites in a tracking-focused method. When GNSS is degraded or unavailable, the vehicle then solely uses the LEO satellites it was previously tracking for navigating its own trajectory. During these instances, STAN's estimate of the LEO satellites' states often diverges and produces inconsistent filter results for the reasons explained in the previous section. By employing machine learning, the aim is to improve the filter's ability to estimate the LEO satellite positions. Machine learning models possess the ability to learn complex nonlinear dynamics models with high levels of uncertainty (cf. (6)), and make accurate predictions at a fraction of the computational cost of comparable orbit propagation methods. During times of GNSS availability, the machine learning model will be trained on the data as the vehicle tracks the LEO satellites, and after GNSS is no longer available, the machine learning aided LEO propagation model will produce predictions of the LEO satellite states, leading to a higher degree of accuracy in the vehicle's navigation performance.

In this paper, the focus is to use machine learning to predict LEO satellite positions, which would improve the navigation performance under the STAN framework. For this reason, supervised learning for time-series regression is employed via a time delay neural network (TDNN). The proposed framework will be referred to as EKF-TDNN-STAN. Neural networks are collections of layers with nodes — or neurons — that are fed input data, which in turn learn trends in the data, and attempt to produce output data. Essentially, each layer takes in inputs from previous layers if available, and uses weights at each node, which are then summed up and passed through an activation function. The network learns the model via a predefined algorithmic update of the weights for each supervised input sample, which later predicts the output of unsupervised inputs. In orbital models, the prediction relies on both present and past inputs, which makes TDNNs an attractive design for this specific problem, where TDNNs posses specific delay features for information from past inputs to persistence and influence the prediction of future outputs. Furthermore, during a closed-loop implementation, TDNN can feed its output prediction back into the network to influence the prediction at future time steps. The proposed TDNN network was trained using the backprogation algorithm and the mean-squared error (MSE) as a performance measure. Furthermore, to compare the TDNN performance to a baseline, an autoregressive model is employed to predict the LEO satellite positions. One noteable drawback of machine learning methods is the computational requirement of the data used and the training time. Although this paper focuses on a performance comparison between different methods, a comprehensive comparison including computational cost is an area of further study.

4. Experimental Results

This section gives an overview of the scenario studied in this paper, presents details about the parameters and training of the TDNN, and compares the navigation performance of a ground vehicle with the proposed EKF-TDNN-STAN with two LEO satellites versus an EKF-STAN.

Scenario Overview

The data presented in this section was taken from experiments conducted with a ground vehicle navigating with two LEO satellites from the Orbcomm constellation. The Orbcomm satellites are part of a communication satellite constellation that also transmit their positions from on-board GNSS receivers. During its 258-second trajectory, the ground vehicle received signals from two Orbcomm satellites and decoded the positions of satellites while also making Doppler measurements from the satellites' signals. These decoded positions were used as the ground truth for the LEO satellite trajectories during the training of the neural network. GNSS signals were artificially cut for the last 30 seconds of the vehicle's trajectory. The training period might seem short for such an application; however, this should be sufficient to learn a model that performs well for a short period of time (e.g, 30 seconds) and shows the potential of the approach. Figure 2 depicts the implementation of the machine learning algorithm into the STAN framework. The inputs of the neural network are the t3-D positions of each satellite expressed in the Earth-centered, Earth-fixed (ECEF) coordinate frame, while the outputs are predictions of the satellite positions one time step ahead. After GNSS signals were cut off, the neural network transitioned to a closed-loop mode where it continually predicted the LEO satellite positions one time-step ahead while using its own predictions as feedback inputs.

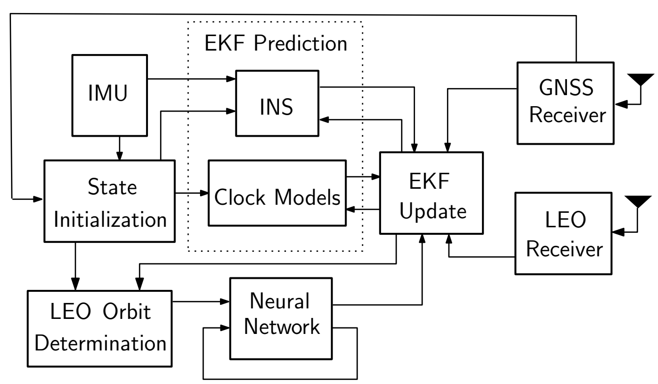

Figure 2. EKF-TDNN-STAN framework that uses a neural network to predict LEO satellite positions.

Model Hyperparameters

The hyperparameters of a machine learning model are used to control the learning process of the model, as opposed to the weights that the model attempts to optimize during training. The specific hyperparameters employed greatly affect the learning result and thus a study to determine the optimal settings must be conducted. Some hyperparameters of interest include: (a) *epoch size*: the number of times the learning algorithm will process the entire set of training data; (b) *batch size*: the number of data samples that will be processed before updating the internal model parameters; (c) *number of layers*:

Authorized licensed use limited to: ISRO Telemetry Tracking and Command Network. Downloaded on May 11,2023 at 11:39:21 UTC from IEEE Xplore. Restrictions apply.

defines the depth of the network, which affects the model's learning ability; (d) *number of neurons*: the number of nodes in a specific layer of the model, which influences the learning capacity of the network; and (e) *time step delays*: a specific parameter to TDNN that specifies how many time-steps the model will look backwards while making its predictions. Activation functions also play an important role in machine learning models. They perform a mathematical operation on the output of each neuron of the model and dictate what values are passed throughout the model. For this work, the activation function used is the hyperbolic tangent sigmoid function. The model hyperparameters chosen after tuning the network are shown in Table 1.

Table 1. Model Hyperparameters

Hyperparameter	Value
Epoch size	1000
Batch size	1
Layers	1
Neurons	20
Time step delays	15

Training and Validation Techniques

For this experiment, the training and validation data are provided during times of GNSS availability, and the testing data is the recorded data after GNSS signals are artificially cut off. This allows the model to use the collected data from when a navigating vehicle knows its own position to a high degree of accuracy to continually train and learn the LEO satellite trajectories. Several learning curves are used to measure the neural network's performance to avoid underfitting (when the model fails to learn the training data and thus more learning could be done) and overfitting (when the model learns the training data so well that it cannot generalize the validation data and results of the test data are poor). The technique of regularization is applied to keep the model weights stable and avoid issues of overfitting. The optimizing function used is the Levenberg-Marquardt backpropagation, which is responsible for updating the weights and biases of the model after each batch. Validation techniques are important to provide ways to validate the model's performance. In this time-series regression problem, two validation techniques are utilized: test-train splitting and autoregressive forecasting.

To serve as a baseline performance measure, an autoregressive model was fit for the prediction of the LEO satellite positions. The goal is to predict the satellite positions using a linear function that contains a combination of the current and past positions. The number of past time steps, or lag variables, to incorporate in the training was optimized to the value that produced the lowest total root-mean squared error (RMSE). The autoregressive model was fit using the training set of LEO satellite positions and the RMSEs were calculated with the remaining test set (final 30 seconds) and are shown in Table 2.

Table 2. Autoregressive Model Performance

Performance Measure	LEO 1	LEO 2
RMSE (km)	1.28	1.38
Final Error (km)	1.37	1.29

Comparative Navigation Results

After the TDNN was trained with the data during the time when GNSS signals were available, the network transitioned to a closed-loop mode to make future predictions. Figure 3 shows the true LEO satellite trajectories, derived from the Orbcomm on-board GNSS receivers, versus the TDNN's prediction of the LEO satellite trajectories during the last 30 seconds of the data. It is difficult to see due to the scale of the image, but the neural network's prediction falls very close to the LEO satellite ground truth trajectory. Table 3 compares the EKF-STAN results versus the EKF-TDNN-STAN, where it is noted that both prediction algorithms perform significantly better than the autoregressive baseline in Table 2. Figures 4 and 5 show the error residuals for both model's predictions for Orbcomm satellites 1 and 2 in their body frames, respectively. It is important to note that the EKF-STAN framework's prediction for the LEO satellites frequently violates the $\pm 3\sigma$ bounds due to filter inconsistency. The oscillatory error is observed is typical for the EKF; however, it is important to stress that in the long-term this diverges rapidly, and for this application, the focus is on short time periods of GNSS-unavailability. Having an alternative method of estimating LEO satellites, like neural networks, can play an important role in improving the navigation performance of the vehicle.

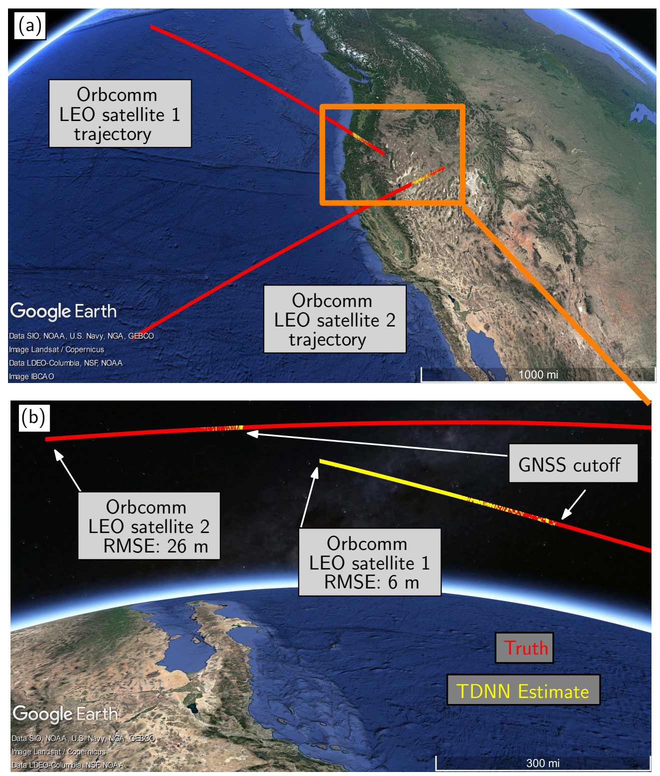

Figure 3. Experimental results showing (a) the trajectory of the 2 Orbcomm LEO satellites, (b) zoom of the TDNN's predictions (yellow) versus the truth trajectories (red) tracked by a ground vehicle without GNSS for 30 seconds. Map data: Google Earth.

Next, the effect of improving the LEO satellite position estimates on the vehicle's navigation performance is analyzed. Figure 6 shows the vehicle's true trajectory along a highway in Irvine, California, USA, compared to estimates from the original EKF-STAN framework and the proposed

Authorized licensed use limited to: ISRO Telemetry Tracking and Command Network. Downloaded on May 11,2023 at 11:39:21 UTC from IEEE Xplore. Restrictions apply.

EKF-TDNN-STAN framework. The results are summarized in Table 4. It is evident that having more accurate predictions of the LEO satellites leads to better navigation performance for the ground vehicle. With further model tuning and more training data, the neural network results could be even further improved. Any minor improvement in vehicle navigation is important for safety and the future implantation of autonomous systems.

Table 3. LEO Satellite Prediction Performance

Performance Measure	LEO 1	LEO 2
EKF-STAN RMSE (m)	71	26
EKF-TDNN-STAN RMSE (m)	6	26

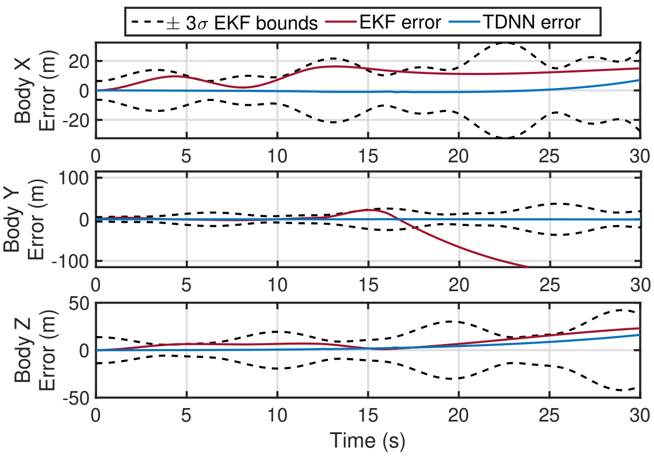

Figure 4. Prediction of Orbcomm LEO Satellite 1: EKF $\pm 3\sigma$ estimation error bounds of the satellite along with EKF error (black) and TDNN prediction error (blue).

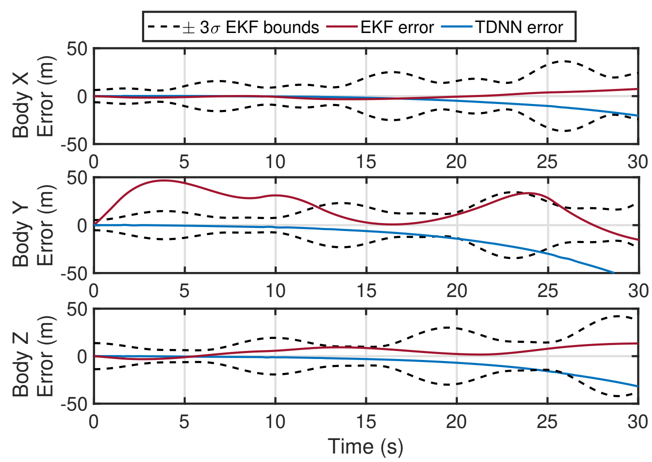

Figure 5. Prediction of Orbcomm LEO Satellite 2: EKF $\pm 3\sigma$ estimation error bounds of the satellite along with EKF error (black) and TDNN prediction error (blue).

Table 4. Ground Vehicle Navigation Performance

Errors	EKF-STAN	EKF-TDNN-STAN
RMSE (m)	10.6	6.6
Final Error (m)	24	16

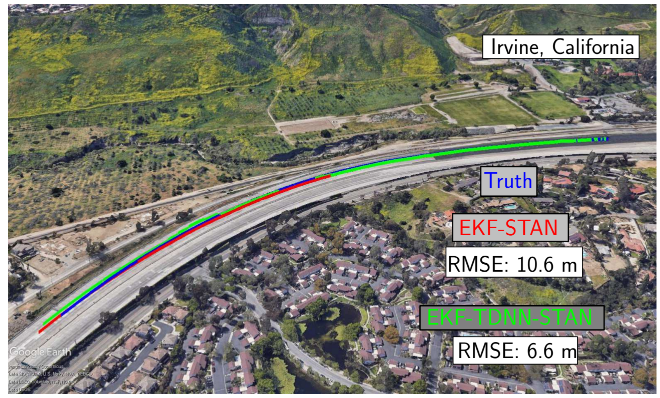

Figure 6. Experimental results showing the trajectory of a ground vehicle truth navigating without GNSS for 30 seconds. The truth (white) is compared to the EKF-STAN estimate (red) and the EKF-TDNN-STAN estimate (yellow). Map data: Google Earth.

5. CONCLUSION

This paper proposed the addition of a neural network to the STAN framework to reduce errors in tracking LEO satellite positions, which effectively improves a vehicle's navigation performance. A TDNN with 20 neurons and 15 time step delays using a backpropagation algorithm to update model weights and biases was developed. Experiments were conducted with a ground vehicle navigating with Doppler measurements drawn from two Orbcomm LEO satellites, where GNSS signals were artificially cut for 30 seconds. The training data for the machine learning model were determined from the satellites' onboard GNSS receivers which broadcast signals decoded by the vehicle. The performance of the TDNN in tracking the LEO satellite positions was compared to an autoregressive model and a traditional LEO propagation model. The neural network aided STAN framework, called EKF-TDNN-STAN, improved the conventional EKF-STAN framework's performance. The EKF-STAN achieved a ground vehicle 3-D position RMSE of 10.6 m, while the two LEO satellites were tracked with 3-D position RMSE of 71 m and 26 m, respectively. In contrast, the proposed EKF-TDNN-STAN framework achieved a ground vehicle 3-D position root RMSE of 6.6 m, while the two LEO satellites were tracked with 3-D position RMSE of 6 m and 26 m, respectively.

ACKNOWLEDGMENTS

This work was supported in part by the Office of Naval Research (ONR) under Grant N00014-19-1-2511 and in part by the National Science Foundation (NSF) under Grant 1929965

REFERENCES

[1] UCS, "UCS satellite database," https://www.ucsusa.org/resources/satellite-database, December 2019.

[2] T. Reid, T. Walter, P. Enge, D. Lawrence, H. Cobb, G. Gutt, M. O'Conner, and D. Whelan, "Position, navigation, and timing technologies in the 21st century," J. Morton, F. van Diggelen, J. Spilker, Jr., and B. Parkinson, Eds. Wiley-IEEE, 2021, vol. 2, ch. 43: Navigation from low Earth orbit – Part 1: Concept, Current Capability, and Future Promise, pp. 1359–1379.

Authorized licensed use limited to: ISRO Telemetry Tracking and Command Network. Downloaded on May 11,2023 at 11:39:21 UTC from IEEE Xplore. Restrictions apply.

[3] Z. Kassas, "Position, navigation, and timing technologies in the 21st century," J. Morton, F. van Diggelen, J. Spilker, Jr., and B. Parkinson, Eds. Wiley-IEEE, 2021, vol. 2, ch. 43: Navigation from low Earth orbit – Part 2: models, implementation, and performance, pp. 1381–1412.

[4] Z. Kassas, "Collaborative opportunistic navigation," *IEEE Aerospace and Electronic Systems Magazine*, vol. 28, no. 6, pp. 38–41, 2013.

[5] D. Lawrence, H. Cobb, G. Gutt, M. OConnor, T. Reid, T. Walter, and D. Whelan, "Navigation from LEO: Current capability and future promise," *GPS World Magazine*, vol. 28, no. 7, pp. 42–48, July 2017.

[6] T. Reid, A. Neish, T. Walter, and P. Enge, "Broadband LEO constellations for navigation," *NAVIGATION, Journal of the Institute of Navigation*, vol. 65, no. 2, pp. 205–220, 2018.

[7] Z. Kassas, J. Khalife, M. Neinavaie, and T. Mortlock, "Opportunity comes knocking: overcoming GPS vulnerabilities with other satellites' signals," *Inside Unmanned Systems Magazine*, pp. 30–35, June/July 2020.

[8] North American Aerospace Defense Command (NORAD), "Two-line element sets," http://celestrak.com/NORAD/elements/.

[9] J. Vetter, "Fifty years of orbit determination: Development of modern astrodynamics methods," *Johns Hopkins APL Technical Digest*, vol. 27, no. 3, pp. 239–252, November 2007.

[10] J. Khalife, M. Neinavaie, and Z. Kassas, "Navigation with differential carrier phase measurements from megaconstellation LEO satellites," in *Proceedings of IEEE/ION Position, Location, and Navigation Symposium*, April 2020, pp. 1393–1404.

[11] M. Tanda, "Blind symbol-timing and frequency-offset estimation in OFDM systems with real data symbols," *IEEE Transactions on Communications*, vol. 52, no. 10, pp. 1609–1612, October 2004.

[12] G. Gao, "Towards navigation based on 120 satellites: Analyzing the new signals," Ph.D. dissertation, Stanford University, 2008.

[13] T. Zhang, S. Dai, W. Zhang, G. Ma, and X. Gao, "Blind estimation of the PN sequence in lower SNR DS-SS signals with residual carrier," *Digital Signal Processing*, vol. 22, no. 1, pp. 106–113, 2012.

[14] J. Khalife, M. Neinavaie, and Z. Kassas, "Blind Doppler estimation from LEO satellite signals: A case study with real 5G signals," in *Proceedings of ION GNSS Conference*, September 2020, pp. 3046–3054.

[15] M. Neinavaie, J. Khalife, and Z. Kassas, "Blind opportunistic navigation: Cognitive deciphering of partially known signals of opportunity," in *Proceedings of ION GNSS Conference*, September 2020, pp. 2748–2757.

[16] M. Neinavaie, J. Khalife, and Z. Kassas, "Blind Doppler tracking and beacon detection for opportunistic navigation with LEO satellite signals," in *Proceedings of IEEE Aerospace Conference*, March 2021, accepted.

[17] Z. Kassas, J. Morales, and J. Khalife, "New-age satellite-based navigation – STAN: simultaneous tracking and navigation with LEO satellite signals," *Inside GNSS Magazine*, vol. 14, no. 4, pp. 56–65, 2019.

[18] C. Ardito, J. Morales, J. Khalife, A. Abdallah, and Z. Kassas, "Performance evaluation of navigation using LEO satellite signals with periodically transmitted satellite positions," in *Proceedings of ION International Technical Meeting Conference*, 2019, pp. 306–318.

[19] J. Morales, J. Khalife, and Z. Kassas, "Simultaneous tracking of Orbcomm LEO satellites and inertial navigation system aiding using Doppler measurements," in *Proceedings of IEEE Vehicular Technology Conference*, April 2019, pp. 1–6.

[20] J. Morales, J. Khalife, U. Santa Cruz, and Z. Kassas, "Orbit modeling for simultaneous tracking and navigation using LEO satellite signals," in *Proceedings of ION GNSS Conference*, September 2019, pp. 2090–2099.

[21] Z. Kassas, "Analysis and synthesis of collaborative opportunistic navigation systems," Ph.D. dissertation, The University of Texas at Austin, USA, 2014.

[22] J. Morales, P. Roysdon, and Z. Kassas, "Signals of opportunity aided inertial navigation," in *Proceedings of ION GNSS Conference*, September 2016, pp. 1492–1501.

[23] Z. Kassas, J. Morales, K. Shamaei, and J. Khalife, "LTE steers UAV," *GPS World Magazine*, vol. 28, no. 4, pp. 18–25, April 2017.

[24] J. Morales and Z. Kassas, "Tightly-coupled inertial navigation system with signals of opportunity aiding," *IEEE Transactions on Aerospace and Electronic Systems*, 2020, accepted.

[25] Z. Kassas, J. Khalife, A. Abdallah, and C. Lee, "I am not afraid of the jammer: navigating with signals of opportunity in GPS-denied environments," in *Proceedings of ION GNSS Conference*, 2020, pp. 1566–1585.

[26] M. Braasch, "Inertial navigation systems," in *Aerospace Navigation Systems*. John Wiley & Sons, Ltd, 2016.

[27] J. Farrell and M. Barth, *The Global Positioning System and Inertial Navigation*. New York: McGraw-Hill, 1998.

[28] P. Misra and P. Enge, *Global Positioning System: Signals, Measurements, and Performance*, 2nd ed. Ganga-Jamuna Press, 2010.

[29] J. Khalife and Z. Kassas, "Receiver design for Doppler positioning with LEO satellites," in *Proceedings of IEEE International Conference on Acoustics, Speech and Signal Processing*, May 2019, pp. 5506–5510.

[30] H. Chen, G. Chen, E. Blasch, and K. Pham, "Comparison of several space target tracking filters," in *Proceedings of SPIE*, vol. 7330, 2009, pp. 1–13.

[31] I. Hussein, K. DeMars, C. Fruh, M. Jah, and R. Erwin, "An aegis-fisst algorithm for multiple object tracking in space situational awareness," in *AIAA/AAS Astrodynamics Specialist Conference*, 2012, pp. 4807–4827.

[32] B. Jia, E. Blasch, K. Pham, D. Shen, Z. Wang, X. Tian, and G. Chen, "Space object tracking and maneuver detection via interacting multiple model cubature Kalman filters," in *Proceedings of IEEE Aerospace Conference*, 2015, pp. 1–8.

[33] E. Blasch, M. Pugh, C. Sheaff, J. Raquepas, and P. Rocci, "Big data for space situation awareness," in *Proceedings of SPIE*, vol. 10196, 2017, pp. 1–13.

[34] E. Delande, C. Frueh, J. Franco, J. Houssineau, and D. Clark, "Novel multi-object filtering approach for space situational awareness," *Journal of Guidance, Control, and Dynamics*, vol. 41, no. 1, pp. 59–73, January 2018.

Authorized licensed use limited to: ISRO Telemetry Tracking and Command Network. Downloaded on May 11,2023 at 11:39:21 UTC from IEEE Xplore. Restrictions apply.

[35] B. Tapley, B. Schutz, and G. Born, *Statistical Orbit Determination*. Burlington, MA: Elsevier Academic Press, 2004.

[36] D. Vallado, "An analysis of state vector propagation using differing flight dynamics programs," in *Proceedings of the AAS Space Flight Mechanics Conference*, vol. 120, January 2005.

[37] A. Rich, "Investigating analytical and numerical methods to predict satellite orbits using two-line element sets," Master's thesis, Air Force Institute of Technology, Wright-Patterson Air Force Base, Ohio, USA, 2017.

[38] C. Levit and W. Marshall, "Improved orbit predictions using two-line elements," *Advances in Space Research*, vol. 47, no. 7, pp. 1107–1115, 2011.

[39] S. Shuster, "A survey and p y and performance analysis of orbit pr formance analysis of orbit propagators for LEO, GEO, and highly elliptical orbits," Master's thesis, Utah State University, Utah, USA, 2017.

[40] Y. Zhao, F. Yu, and N. Xu, "PPP augmentation and real-time precise orbit determination for LEO satellites," in *Proceedings of the Chinese Control Conference*, 2017, 5937–5941.

[41] A. Hauschild, J. Tegedor, O. Montenbruck, H. Visser, and M. Markgraf, "Precise onboard orbit determination for LEO satellites with real-time orbit and clock corrections," in *Proceedings of ION GNSS Conference*, September 2016, 3715–3723.

[42] P. Giordano, P. Z. M. Otten, and C. Massimo, "P2OD: real-time precise onboard orbit determination for LEO satellites," in *Proceedings of ION GNSS Conference*, September 2017, 1754–1771.

[43] B. Lee, W. Kim, J. Lee, and Y. Hwang, "Machine learning approach to initial orbit determination of unknown LEO satellites," in *Proceedings of AIAA SpaceOps Conference*, 2018, pp. 1–11.

[44] S. Sharma and J. Cutler, "Robust orbit determination and classification: A learning theoretic approach," *IPN Progress Report*, pp. 42–203, 2015.

[45] F. Feng, Y. Zhang, H. Li, Y. Fang, Q. Huang, and X. Tao, "A novel space-based orbit determination method based on distribution regression and its sparse solution," *IEEE Access*, vol. 7, pp. 133 203–133 217, 2019.

[46] D. Shen, J. Lu, G. Chen, E. Blasch, C. Sheaff, M. Pugh, and K. Pham, "Proceedings of methods of machine learning for space object pattern classification," in *IEEE National Aerospace and Electronics Conference*, 2019, pp. 565–572.

[47] B. Li, J. Huang, Y. Feng, F. Wang, and J. Sang, "A machine learning-based approach for improved orbit predictions of LEO space debris with sparse tracking data from a single station," *IEEE Transactions on Aerospace and Electronic Systems*, 2020.

[48] H. Peng and X. Bai, "Limits of machine learning approach on improving orbit prediction accuracy using support vector machine," in *Proceedings of the Advanced Maui Optical and Space Surveillance*, 2017, pp. 1–22.

[49] H. Peng and X. Bai, "Comparative evaluation of three machine learning algorithms on improving orbit prediction accuracy," *Astrodynamics*, vol. 3, no. 4, pp. 325–343, 2019.

[50] H. Peng and X. Bai, "Machine learning approach to improve satellite orbit prediction accuracy using publicly available data," *The Journal of the Astronautical Sciences*, vol. 67, no. 2, pp. 762–793, 2020.

[51] R. Mital, K. Cates, J. Coughlin, and G. Ganji, "A machine learning approach to modeling satellite behavior," in *Proceedings of IEEE International Conference on Space Mission Challenges for Information Technology*, 2019, pp. 62–69.

[52] N. Salleh, S. Yuhaniz, N. Azmi, and S. Sabri, "Enhancing simplified general perturbations-4 model for orbit propagation using deep learning: a review," in *Proceedings of the International Conference on Software and Computer Applications*, 2019, 5937–5941.

BIOGRAPHY

Trier R. Mortlock *is a Ph.D. student in the Department of Mechanical and Aerospace Engineering at the University of California, Irvine. He received a B.S. in Mechanical Engineering from the University of California, Berkeley. He serves in the U.S. Army Reserve serving as a Cyber Operations Officer. His current research interests include cyber-physical systems, satellite-based navigation, and situational awareness in dynamic uncertain environments.*

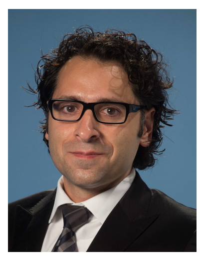

Zaher (Zak) M. Kassas *is an associate professor at the University of California, Irvine and director of the Autonomous Systems Perception, Intelligence, and Navigation (ASPIN) Laboratory. He is also director of the U.S. Department of Transportation Center: CARMEN (Center for Automated Vehicle Research with Multimodal AssurEd Navigation), focusing on navigation resiliency and security of highly automated transportation systems. He received a B.E. in Electrical Engineering from the Lebanese American University, an M.S. in Electrical and Computer Engineering from The Ohio State University, and an M.S.E. in Aerospace Engineering and a Ph.D. in Electrical and Computer Engineering from The University of Texas at Austin. He received the 2018 National Science Foundation (NSF) Faculty Early Career Development Program (CAREER) award, and 2019 Office of Naval Research (ONR) Young Investigator Program (YIP) award. He is a recipient of the 2018 IEEE Walter Fried Award, 2018 Institute of Navigation (ION) Samuel Burka Award, and 2019 ION Col. Thomas Thurlow Award. He is an Associate Editor for the IEEE Transactions on Aerospace and Electronic Systems and the IEEE Transactions on Intelligent Transportation Systems. His research interests include cyber-physical systems, estimation theory, navigation systems, autonomous vehicles, and intelligent transportation systems.*

Authorized licensed use limited to: ISRO Telemetry Tracking and Command Network. Downloaded on May 11,2023 at 11:39:21 UTC from IEEE Xplore. Restrictions apply.